450. *Peroxy-complexes of Inorganic Ions in Hydrogen Peroxide–Water Mixtures. Part I. Decomposition by Ferric Ions.*

By T. J. Lewis, D. H. Richards, and D. A. Salter.

Study of the ferric iron–hydrogen peroxide–water system by spectrophotometry and measurement of oxygen evolution have provided evidence for the existence of species $Fe^{3+}(H_2O)_5(H_2O_2)$ and $Fe^{3+}(H_2O)_5O_2H^-$; their constants of formation have been determined at an ionic strength 0·5 and 22°, as has that of $Fe^{3+}(H_2O)_5OH^-$. Work in highly concentrated peroxide suggests the presence of a species $Fe^{3+}(H_2O)_4(H_2O_2)O_2H^-$ although the concentration of $Fe^{3+}(H_2O)_4(H_2O_2)_2$ is thought to be negligible.

These species have been shown to be responsible for the catalytic activity of ferric ions in hydrogen peroxide. The kinetics of decomposition have been confirmed as mixed unimolecular and bimolecular with respect to iron, and six rate constants have been estimated which describe the catalytic activity over a wide range of peroxide and hydrogen-ion concentrations.

THE catalytic decomposition of hydrogen peroxide by ferric ions has been studied by a great many authors,[1] but generally only for dilute peroxide solutions. For this region the decomposition mechanism of Barb *et al.*[2] seems to explain the facts most completely. Evans, George, and Uri[3] and, more recently, Kremer and Stein[4] studied the system spectroscopically and gave evidence for the formation of $Fe^{3+}O_2H^-$ ions. The last authors correlated the presence of this ion with the rate of decomposition of the hydrogen peroxide. However, they postulated the existence, in exceedingly dilute peroxide, of two forms of this species and introduced non-steady-state kinetics to explain their results.

For more concentrated peroxide, notable papers have appeared by Wynne-Jones and his school.[5,6] These authors,[5] studying the system by measurement of oxygen evolution, explained their results by postulating the equilibria:

$$Fe^{3+}(H_2O)_6 + H_2O_2 \rightleftharpoons H_2O + Fe^{3+}(H_2O)_5(H_2O_2) \longrightarrow$$
$$\longrightarrow \text{Products}$$
$$Fe^{3+}(H_2O)_5(H_2O_2) + H_2O_2 \rightleftharpoons H_2O + Fe^{3+}(H_2O)_4(H_2O_2)_2 \longrightarrow$$
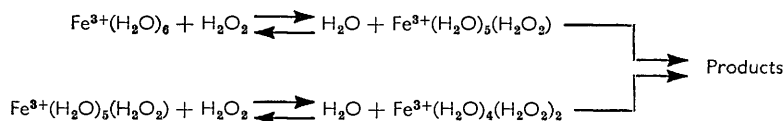
The complexity of the decomposition was further shown by the observation that the kinetics were partly bimolecular with respect to iron. The experimental results were explained by the proposed mechanism extremely well at pH 2, but the effect of acidity changes on the system was not studied although it is known that the catalytic activity of ferric solutions is strongly dependent on the hydrogen-ion concentration. To account for this acid-dependence these authors postulated that the decomposition proceeded *via* the dissociated ferric species, and in the later paper[6] spectroscopic evidence was given which confirmed the work of Evans, George, and Uri and showed that their species could be produced by the mechanism given above. Again, however, no variation of acid strength was reported and therefore the equilibrium constants could not be quantitatively assessed.

Although the work of Wynne-Jones's school leaves little doubt that their mechanism is essentially correct, the kinetic picture cannot be fully revealed at constant acid strength. We have therefore re-examined the system at variable acidity, using both spectrophotometry and measurements of gas evolution.

[1] Reviews, Baxendale, *Adv. Catalysis*, 1952, **4**, 31; Weiss, *ibid.*, p. 343; Uri, *Chem. Rev.*, 1952, **50**, 375.
[2] Barb, Baxendale, George, and Hargrave, *Trans. Faraday Soc.*, 1951, **47**, 462, 591.
[3] Evans, George, and Uri, *Trans. Faraday Soc.*, 1949, **45**, 230.
[4] Kremer and Stein, *Trans. Faraday Soc.*, 1959, **55**, 959.
[5] Jones, Kitching, Tobe, and Wynne-Jones, *Trans. Faraday Soc.*, 1959, **55**, 79.
[6] Haggett, Jones, and Wynne-Jones, *Discuss. Faraday Soc.*, 1960, **29**, 153.

Because of the complexity of the kinetics of decomposition, as demonstrated by the oxygen evolution, it appeared more fruitful to study the solutions spectroscopically first so that the ferric species present could be identified and the equilibrium constants determined. These results should then have a direct bearing on the interpretation of the decomposition experiments. The spectroscopic results will therefore be considered first.

EXPERIMENTAL

Materials.—Ferric perchlorate was used throughout as source of ferric ions. It was prepared by dissolving pure iron powder in a known amount of " AnalaR " perchloric acid. The resulting solution was oxidised by hydrogen peroxide to form a ferric perchlorate solution. Water was distilled off under a vacuum until crystals separated. These were quickly filtered off and dried at 60° for 48 hr. *in vacuo.* They were stored in a blackened vacuum-desiccator which was opened only under dry nitrogen. Analysis showed the composition to be $Fe(ClO_4)_3,6H_2O$.

Sodium perchlorate supplied by Hopkin and Williams gave inconsistent results in preliminary experiments although the material was recrystallised before use. We suspect that this was due to the presence of small amounts of other anions such as sulphate or phosphate which readily complex with ferric ions. The most consistent results were obtained when the sodium perchlorate was prepared by neutralising " AnalaR " sodium hydroxide with " AnalaR " perchloric acid (external indicator).

Hydrogen peroxide free from stabiliser was supplied by Laporte Chemicals Ltd. and was distilled before use.

Conductivity water was used throughout.

Analyses.—Ferric perchlorate was analysed by using the stannous chloride reduction method for ferric ions [7] and titrating the total perchlorate, whether present as $HClO_4$ or $Fe(ClO_4)_3$, at 60° with alkali (phenolphthalein indicator [8]).

Hydrogen peroxide solutions containing ferric ions were analysed by terminating catalysis with sulphuric acid and titrating the solution with potassium permanganate.

Concentration Units.—In water–hydrogen peroxide mixtures the number of moles of solvent per unit volume varies with solvent composition. Thus, if solute is introduced into various solvent mixtures at constant molarity, its concentration expressed in mole fractions increases with the concentration of peroxide present. It is therefore important to decide which concentration unit is most suitable for use in the present case. This situation has been discussed at length by Jones *et al.*[5] but no decision can be made on purely theoretical grounds. These authors concluded that their experimental results were best described in mole fraction units. We have also found mole fractions to give us the better agreement with theory and have accordingly used them for all calculations. Molarity terms are, however, more convenient in preparation of solutions and we have retained these units where concentrations are mentioned in the purely descriptive passages of the text. These two units may be interconverted by using the density data determined by Easton, Mitchell, and Wynne-Jones.[9]

Techniques.—Solutions were prepared in series at constant hydrogen peroxide concentration and adjusted acidity between $C_{H^+} = 1 \times 10^{-2}$ and 50×10^{-2} g.-ion/l. In this range the decomposition has been shown to be homogeneous.[10] Throughout our work the ionic strength was maintained at 0·5 by addition of sodium perchlorate.

Spectroscopic measurements were performed on a Unicam S.P. 500 spectrophotometer with 4 cm. matched glass cells. As this instrument possesses no temperature-control system, the measurements were made at room temperature although effort was made to restrict the cell temperature to $22° \pm 1°$. Measurements were greatly hampered by repeated formation of oxygen bubbles, especially in solutions of more concentrated peroxide. This was minimised by introducing the solutions into the optical cells, placing the cells in the cell-holder, and degassing the solutions in a vacuum-desiccator. Air was then allowed to re-enter the desiccator immediately before the measurement, and the optical densities were measured before the

[7] Vogel, " A Textbook of Quantitative Inorganic Analysis," Longmans, Green & Co., London, 1947, p. 565.
[8] Schumb and Sweetser, *J. Amer. Chem. Soc.*, 1935, **57**, 871.
[9] Easton, Mitchell, and Wynne-Jones, *Trans. Faraday Soc.*, 1952, **48**, 796.
[10] Banfield and Hilden, E.R.D.E., E.M.R. Report No. 2/EMR/53.

solutions had again become saturated with oxygen. For the more concentrated peroxide solutions, the rate of gas evolution was such that saturation was reached too quickly for precise measurements to be made and the accuracy of the results obtained at these concentrations is therefore suspect. Small corrections were made to the recorded optical densities for the measured differences in absorption between the cells when filled with distilled water.

Gas-evolution experiments were carried out in a thermostat-bath at 22° in order to compare the results directly with those obtained spectroscopically. The rates of oxygen evolution were measured with automatic self-levelling gas-burettes designed here,[11] which enabled the decomposition rates of eight solutions to be measured simultaneously.

The ferric solutions for the spectroscopic work were prepared directly from the crystals and not from a more concentrated stock solution as it has been shown [12] that, in aqueous ferric solutions more concentrated than 10^{-3}M, polynuclear species are formed which only very slowly disappear on subsequent dilution. However, solutions prepared in this manner and from stock solutions showed substantially the same rate of evolution of oxygen. The bulk of the oxygen results were therefore obtained from solutions prepared from stock, in view of the greater accuracy of reproducing standard iron concentrations from stock solutions than from hygroscopic crystals.

SPECTROSCOPIC ANALYSIS

Theory.—Let us assume the annexed equilibria to be present in the ferric–hydrogen peroxide system.

$$\mathrm{Fe^{3+}(H_2O)_6 + HS} \underset{}{\overset{K_1}{\rightleftharpoons}} \mathrm{Fe^{3+}(H_2O)_5OH^- + H_2S^+}$$
$$(C_a - \textstyle\sum C_x)\gamma_a \quad a_{HS} \qquad\qquad a_x \qquad\qquad a_{H^+}$$

$$\mathrm{Fe^{3+}(H_2O)_6 + H_2O_2} \underset{}{\overset{K_2}{\rightleftharpoons}} \mathrm{Fe^{3+}(H_2O)_5(H_2O_2) + H_2O}$$
$$(C_a - \textstyle\sum C_x)\gamma_a \quad a_{H_2O_2} \qquad\qquad a_y \qquad\qquad a_{H_2O}$$

$$\mathrm{Fe^{3+}(H_2O)_5(H_2O_2) + HS} \underset{}{\overset{K_3}{\rightleftharpoons}} \mathrm{Fe^{3+}(H_2O)_5O_2H^- + H_2S^+}$$
$$a_y \qquad\qquad a_{HS} \qquad\qquad a_z \qquad\qquad a_{H^+}$$

$$\mathrm{Fe^{3+}(H_2O)_5(H_2O_2) + H_2O_2} \underset{}{\overset{K_4}{\rightleftharpoons}} \mathrm{Fe^{3+}(H_2O)_4(H_2O_2)_2 + H_2O}$$
$$a_y \qquad\qquad a_{H_2O_2} \qquad\qquad a_v \qquad\qquad a_{H_2O}$$

$$\mathrm{Fe^{3+}(H_2O)_4(H_2O_2)_2 + HS} \underset{}{\overset{K_5}{\rightleftharpoons}} \mathrm{Fe^{3+}(H_2O)_4(H_2O_2)O_2H^- + H_2S^+}$$
$$a_v \qquad\qquad a_{HS} \qquad\qquad a_w \qquad\qquad a_{H^+}$$
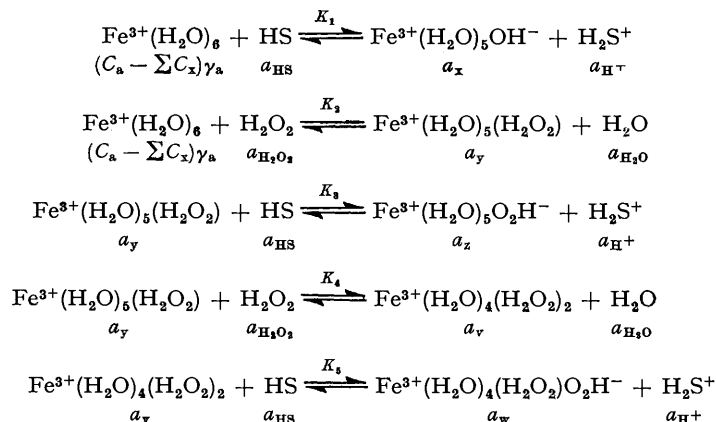
In these equations a represents the activity of the species considered, γ its activity coefficient with respect to an activity coefficient in pure water of unity, and C its concentration. HS represents the solvent, the composition of which is variable.

From these five equations we may show that:

$$C_a - \sum C_x = \frac{C_a a_{H^+}}{\gamma_a\left\{\left(\dfrac{1}{\gamma_a} + \dfrac{K_2\theta}{\gamma_y} + \dfrac{K_2K_4\theta^2}{\gamma_v}\right)a_{H^+} + \left(\dfrac{K_1}{\gamma_x} + \dfrac{K_2K_3\theta}{\gamma_z} + \dfrac{K_2K_4K_5\theta^2}{\gamma_w}\right)a_{HS}\right\}}$$

$$= \frac{C_a a_{H^+}}{\gamma_a M}, \tag{1}$$

Similarly,

$$C_x = \frac{C_a K_1 a_{HS}}{\gamma_x M}; \quad C_y = \frac{C_a K_2 \theta a_{H^+}}{\gamma_y M}; \quad C_z = \frac{C_a K_2 K_3 \theta a_{HS}}{\gamma_z M}; \quad C_v = \frac{C_a K_2 K_4 \theta^2 a_{H^+}}{\gamma_v M}; \quad C_w = \frac{C_a K_2 K_4 K_5 \theta^2 a_{HS}}{\gamma_w M};$$

where $\theta = a_{H_2O_2}/a_{H_2O}$.

[11] Dedman, E.R.D.E. Technical Memorandum No. 1/M/62.
[12] Siddall and Vosburgh, *J. Amer. Chem. Soc.*, 1951, **73**, 4270.

If we assume that the absorptions at a given wavelength are proportional to the concentration of the species present, then the optical density per unit cell length is given by

$$d = \varepsilon_a(C_a - \sum C_x) + \varepsilon_x C_x + \varepsilon_y C_y + \varepsilon_z C_z + \varepsilon_v C_v + \varepsilon_w C_w;$$

so that

$$\frac{d}{C_a} = \frac{\left(\dfrac{\varepsilon_a}{\gamma_a} + \dfrac{\varepsilon_y K_2\theta}{\gamma_y} + \dfrac{\varepsilon_v K_2 K_4 \theta^2}{\gamma_v}\right)a_{H^+} + \left(\dfrac{\varepsilon_x K_1}{\gamma_x} + \dfrac{\varepsilon_z K_2 K_3 \theta}{\gamma_z} + \dfrac{\varepsilon_w K_2 K_4 K_5 \theta^2}{\gamma_w}\right)a_{HS}}{\left(\dfrac{1}{\gamma_a} + \dfrac{K_2\theta}{\gamma_y} + \dfrac{K_2 K_4 \theta^2}{\gamma_v}\right)a_{H^+} + \left(\dfrac{K_1}{\gamma_x} + \dfrac{K_2 K_3 \theta}{\gamma_z} + \dfrac{K_2 K_4 K_5 \theta^2}{\gamma_w}\right)a_{HS}} \qquad (2)$$

If γ_a/γ_m is constant, independent of a_{H^+} at constant θ (where $\gamma_m = \gamma_x$ or γ_y, etc.), then

$$\frac{d}{C_a} = \frac{A a_{H^+} + B}{C a_{H^+} + D} \text{ at constant } \theta \text{ and variable } a_{H^+}, \qquad (3)$$

and, if we consider the optical density d in relation to a standard solution of optical density d_0 and acidity $a^\circ_{H^+}$, we have

$$\frac{d - d_0}{C_a} = \frac{\Delta d}{C_a} = \frac{(BC - AD)\Delta a_{H^+}}{(C a_{H^+} + D)(C a^\circ_{H^+} + D)} \text{ where } \Delta a_{H^+} = a^\circ_{H^+} - a_{H^+},$$

so that

$$\frac{\Delta C_{H^+}}{\Delta d} = \left(C C_{H^+} + \frac{D}{\gamma_{H^+}}\right)\left(\frac{C a^\circ_{H^+} + D}{(BC - AD)C_a}\right). \qquad (4)$$

A plot of $\Delta C_{H^+}/\Delta d$ against C_{H^+} should therefore give a straight line and Intercept/Slope = $K_{sp} = D/C\gamma_{H^+}$ (γ_{H^+} being assumed to be constant at constant θ).

On resubstituting for D and C we obtain

$$K_{sp} = \frac{\dfrac{K_1}{\gamma_x} + \dfrac{K_2 K_3 \theta}{\gamma_z} + \dfrac{K_2 K_4 K_5 \theta^2}{\gamma_w}}{\dfrac{1}{\gamma_a} + \dfrac{K_2\theta}{\gamma_y} + \dfrac{K_2 K_4 \theta^2}{\gamma_v}} \cdot \frac{a_{HS}}{\gamma_{H^+}}. \qquad (5)$$

This analysis is similar to that introduced by Richards and Sykes.[13] It has the advantage that a linear relationship will be obtained regardless of the species which are absorbing in the wave-length range under study.

Because of the similarity of charge and structure one may say as a good approximation that

$$\gamma_x = \gamma_z = \gamma_w, \text{ and } \gamma_a = \gamma_y = \gamma_v,$$

so that

$$K_{sp} = \frac{K_1 + K_2 K_3 \theta + K_2 K_4 K_5 \theta^2}{1 + K_2\theta + K_2 K_4 \theta^2} \cdot \frac{\gamma_a a_{HS}}{\gamma_z \gamma_{H^+}}. \qquad (6)$$

Only the term involving the equilibrium constants would be obtained if changes in the solvent composition had no effect on the stability of the ions involved. The second term allows for changes in the basicity of the medium and the effect of solvent variation on the activities of the ferric species.

It will be found experimentally that the variation of K_{sp} with θ may be completely described by the first term only, *i.e.*, the solvent seems to be behaving ideally. We have observed this effect with other peroxy-acids.[14] Therefore, under these conditions equation (6) reduces to

$$K_{sp} = \frac{K_1 + K_2 K_3 \theta + K_2 K_4 K_5 \theta^2}{1 + K_2\theta + K_2 K_4 \theta^2}. \qquad (7)$$

Lastly, if a wavelength range is selected where only one ionic type absorbs appreciably, then

[13] Richards and Sykes, *J.*, 1960, 3626.
[14] Following papers.

the analysis is simplified. Thus, if we assume that only the dissociated ferric complexes absorb, equation (2) reduces to

$$\frac{d}{C_{a}} = \frac{\left(\dfrac{\varepsilon_{x}K_{1}}{\gamma_{x}} + \dfrac{\varepsilon_{z}K_{2}K_{3}\theta}{\gamma_{z}} + \dfrac{\varepsilon_{w}K_{2}K_{4}K_{5}\theta^{2}}{\gamma_{w}}\right)a_{HS}}{\left(\dfrac{1}{\gamma_{a}} + \dfrac{K_{2}\theta}{\gamma_{y}} + \dfrac{K_{2}K_{4}\theta^{2}}{\gamma_{v}}\right)a_{H^{+}} + \left(\dfrac{K_{1}}{\gamma_{x}} + \dfrac{K_{2}K_{3}\theta}{\gamma_{z}} + \dfrac{K_{2}K_{4}K_{5}\theta^{2}}{\gamma_{w}}\right)a_{HS}}$$

(8)

$$= \frac{B}{Ca_{H^{+}} + D}.$$

Therefore a plot of $1/d$ against $C_{H^{+}}$ gives Intercept/Slope $= K_{sp} = D/C\gamma_{H^{+}}$ as in equation (5).

Results.—Preliminary experiments confirmed that Beer's law was obeyed over an iron concentration range up to 2×10^{-3}M. Optical densities were measured in the wavelength range 450 to 480 mμ for series of solutions at different acidities but constant peroxide concentrations. Over these wavelengths hydrogen peroxide has a negligible absorption. The ferric concentrations in these solutions ranged from 5×10^{-4}M for those containing the highest peroxide concentration to 1×10^{-3}M for the most dilute.

Plots of $\Delta C_{H^{+}}/\Delta d$ against $C_{H^{+}}$ were obtained, which proved to be linear (Fig. 1a), and the
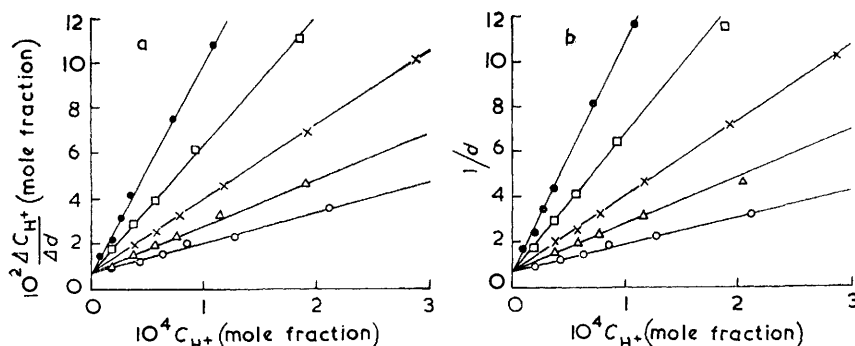
Fig. 1. Plots against $C_{H^{+}}$, at $\mu = 0.5$, and $22°$; $C_{Fe^{3}} = 5.0 \times 10^{-4}$M; $\lambda = 460$ mμ.
(Optical densities measured in 4 cm. cells.)

$\theta = \bigcirc, 0.333; \triangle, 0.233; \times, 0.145; \square, 0.057; \bullet, 0.031.$

K_{sp} values calculated from those graphs were shown to be independent of wavelength and dependent only on the peroxide concentration (Table 1).

TABLE 1.

Effect of wavelength on $10^{5}K_{sp}$ at various values of θ.

mμ \ θ	0.91	0.233	0.077	0.047	mμ \ θ	0.91	0.233	0.077	0.047
450	72.5	25.6	14.8	8.85	470	78.4	25.3	16.6	8.96
455	71.6	26.1	17.5	7.92	475	83.0	26.3	17.4	7.80
460	73.7	26.3	15.8	8.08	480	72.5	25.9	18.5	7.80
465	73.0	25.9	16.6	8.27	Average	72.2	25.9	16.6	8.23

K_{sp} values were determined over a range of peroxide concentrations from 0.05 to 0.75 mole fractions. The graphical linearity indicates that, under the experimental acid conditions $(1—50 \times 10^{-2}$M), there is no significant formation of any doubly ionised ferric species of the type $Fe^{3+}(H_{2}O)_{4}(O_{2}H^{-})_{2}$. The presence of these complexes would result in deviations in the plot owing to the introduction of a $C_{H^{+}}^{2}$ term into the preceding theory.

It was also shown that linear relationships were obtained when $1/d$ was plotted against $C_{H^{+}}$ (Fig. 1b.). Further, the ratio of intercept to slope was, within experimental error, the same as for the previous plot (Table 2).

TABLE 2.

Comparison of K_{sp} obtained at 460 mμ from plots of (a) $\Delta C_{H^+}/\Delta d$ against C_{H^+} and
(b) $1/d$ against C_{H^+}.

θ	0·333	0·233	0·145	0·057	0·031
$10^5 K_{sp}$ (a)	47·0	29·8	19·8	10·8	7·98
$10^5 K_{sp}$ (b)	45·8	31·2	18·6	11·9	8·08

Therefore only the ionised ferric complexes can absorb appreciably between 450 and 480 mμ. Previous work [15] has established the fact that the species $Fe^{3+}(H_2O)_5OH^-$ has its longest-wavelength absorption peak at 300—310 mμ and does not absorb significantly in the visible region. The observed absorptions must consequently be due to $Fe^{3+}(H_2O)_5O_2H^-$ and/or $Fe^{3+}(H_2O)_4(H_2O_2)O_2H^-$.

In order to determine K_1 under these conditions, absorption measurements were carried out in water over the wavelength range 290—330 mμ, 1 cm. in silica cells. Equation (7) at $\theta = 0$ reduces to $K^\circ_{sp} = K_1$ and is therefore a direct measure of K_1. Again, good linear plots were obtained, giving a value of $K_1 = 2·8 \times 10^{-5}$ expressed in mole fractions.

As the concentration of peroxide in the solvent decreases, so the value of K_{sp} decreases
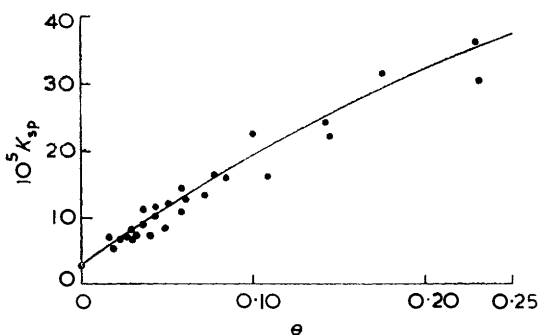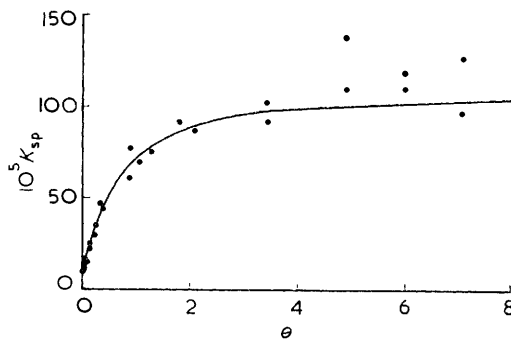
FIGS. 2 and 3. Plots of K_{sp} against θ at $\mu = 0·5$, and 22°. (Curves are calculated values.)

(Figs. 2 and 3). The effect of dilution on the equilibria is to reduce the contribution due to the doubly peroxy-substituted species. At sufficiently dilute peroxide equation (7) must approximate to

$$K_{sp} = (K_1 + K_2 K_3 \theta)/(1 + K_2 \theta). \qquad (9)$$

The graph of K_{sp} against θ at dilute peroxide is shown in Fig. 2. The values of a_{H_2O} and $a_{H_2O_2}$ were calculated for 22° from the thermodynamic data of Scatchard, Kavanagh, and Ticknor.[16]

Now we have shown that, at $\theta = 0$, $K^\circ_{sp} = K_1$, so that, combining this with equation (9), we obtain

$$\frac{\theta}{\Delta K_{sp}} = \frac{1}{K_2(K_3 - K_1)} + \frac{1}{K_3 - K_1} \cdot \theta \text{ (where } \Delta K_{sp} = K_{sp} - K^\circ_{sp}); \qquad (10)$$

thus a plot of $\theta/\Delta K_{sp}$ against θ should be linear over the range of peroxide concentrations where equation (9) still holds. The Slope/Intercept of this plot gives K_2 directly, and K_3 may be determined from the intercept or slope as K_1 has been evaluated.

Such a plot is given in Fig. 4 where the linearity is seen to extend up to $\theta = 2$ or 3, at which point negative deviations begin to appear. From this plot values of $K_2 = 1·8$ and $K_3 = 1·1 \times 10^{-3}$ mole fraction were obtained. At dilute peroxide this plot is very scattered because K_{sp} and K°_{sp} are comparable in this region. Introduction of the equilibrium constant values into equation (9) gave the solid lines in Figs. 2 and 3. It is apparent from these curves that equation (9) is a close approximation to K_{sp}, at least for values of θ less than 2. Above this,

[15] Richards, " Ferric Complexes in Aqueous Solution," Ph.D. Thesis, Wales, 1954.
[16] Scatchard, Kavanagh, and Ticknor, *J. Amer. Chem. Soc.*, 1952, **74**, 3715.

deviations seem to occur which are probably due to the formation of significant amounts of the biperoxy-complex $Fe^{3+}(H_2O)_4(H_2O_2)O_2H^-$. However, this region also coincides with that of the greatest experimental difficulties owing to the increase in bubble formation; consequently, conclusions about trends at these concentrations must be rather uncertain.

From this evidence, however, it is apparent that at least up to medium peroxide concentrations the complex responsible for the measured light absorption is $Fe^{3+}(H_2O)_5O_2H^-$ only. Equation (8) predicts that, from the plot of $1/d$ against C_{H^+}, the reciprocal of the intercept is given by

$$\frac{1}{i_{sp}} = \frac{(\varepsilon_x K_1 + \varepsilon_z K_2 K_3 \theta + \varepsilon_w K_2 K_4 K_5 \theta^2) C_a}{K_1 + K_2 K_3 \theta + K_2 K_4 K_5 \theta^2}.$$

In the wavelength range considered, ε_x is very small, and, if we consider values of θ where $K_2 K_3 \theta \gg K_1$ then this reduces to

$$\frac{1}{i_{sp}} = \frac{(\varepsilon_z K_2 K_3 \theta + \varepsilon_w K_2 K_4 K_5 \theta^2) C_a}{K_2 K_3 \theta + K_2 K_4 K_5 \theta^2} \tag{11}$$

Under conditions where only the monoperoxy-species is present, $1/i_{sp}$ should therefore remain constant, independently of θ, and, if $\varepsilon_z \neq \varepsilon_w$, should change only when a significant
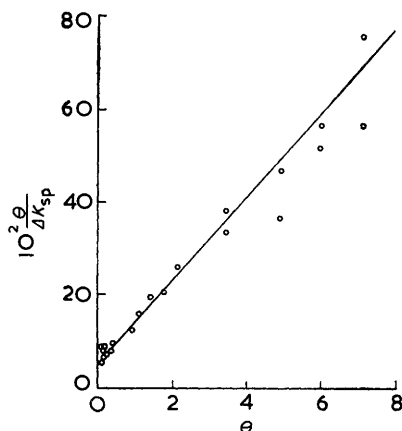
Fig. 4. Plot of $\theta/\Delta K_{sp}$ against θ at $\mu = 0.5$, and $22°$.

amount of the biperoxy-species has been formed. Table 3 lists $1/i_{sp}$ for various values of θ at $C_{Fe^{3+}} = 1 \times 10^{-3}M$ and $450 \, m\mu$.

TABLE 3.

Change of $1/i_{sp}$ with θ.

θ	$1/i$	θ	$1/i$	θ	$1/i$	θ	$1/i$
0·017	2·6	0·038	3·2	0·145	2·9, 3·0	2·22	3·5
0·026	2·6	0·047	2·6	0·233	3·0	3·43	3·6, 3·4
0·029	3·0	0·057	2·9	0·333	3·1	6·0	4·0, 3·7
0·031	2·9	0·077	2·6	0·909	3·2	7·13	4·0, 4·0

$1/i_{sp}$ remains sensibly constant up to $\theta \approx 2$, above which a small increase develops. This indicates, in agreement with the previous observations, that second substitution occurs appreciably only at very high peroxide concentrations. This result is surprising and requires some discussion.

Because of the similarity of structure of the mono- and the di-peroxy-ionised complexes one would expect $K_5 \approx 2K_3 = 2.2 \times 10^{-3}$ mole fraction. If, therefore, K_4 were of the same order as K_2, then appreciable ionisation of the second substituted product should have occurred at moderate peroxide concentrations. It seems difficult to justify a sizable drop in the magnitude of K_5 to account for the experimental findings, and therefore it seems likely that K_4 must be less than K_2 for some reason. A possible explanation may be based on steric hindrance.

The solvating molecules around the ferric ion are distributed at the apices of a regular octahedron. When one of these points is occupied by a peroxide molecule, then a second peroxide molecule will occupy one of two sterically different positions, a *cis*- (which has four equivalent sites) and the *trans*-position. If the introduction of a peroxide into the *cis*-position resulted in appreciable steric hindrance this would make peroxide substitution at any of these sites difficult and therefore drastically reduce K_4. Once substitution had taken place, steric hindrance could be partly relieved by ionisation of one of the peroxide molecules and so K_5 would tend to be greater than $2K_3$. Substitution at the *trans*-position should introduce little more steric hindrance than in the substitution of the original peroxide and the replacement constant per site should be similar. However, from statistical considerations, the constants per ferric ion should differ by a factor of six so that *trans*-substitution should give $K_4 \approx \frac{1}{6}K_2$ and $K_5 \approx 2K_3$. Consequently, at high peroxide concentrations where a significant amount of $Fe^{3+}(H_2O)_4(H_2O_2)O_2H^-$ seems to be present, the concentration of $Fe^{3+}(H_2O)_4(H_2O_2)_2$ is probably still very small.

A summary of the equilibrium constants determined by spectrophotometric analysis is given in Table 6.

OXYGEN EVOLUTION ANALYSIS

Theory.—Preliminary experiments indicated that the rate of decomposition was not proportional to the ferric concentration, and further experiments confirmed the observation by Jones *et al.*[5] that the decomposition kinetics were of the combined first- and second-order with respect to iron. Investigations on the effect of acidity on the rate of oxygen evolution showed an inverse dependence, suggesting that the prime catalytically active ferric complexes are the dissociated peroxy-species. The decomposition rate is also a direct function of the peroxide concentration. The kinetic expression must therefore be of the form:

$$-\mathrm{d}C_{H_2O_2}/\mathrm{d}t = f(\theta, C_{H^+})C_a + \Phi(\theta, C_{H^+})C_a^2$$

From these observations plus the spectroscopic evidence, the following reaction scheme seems to be the most general:
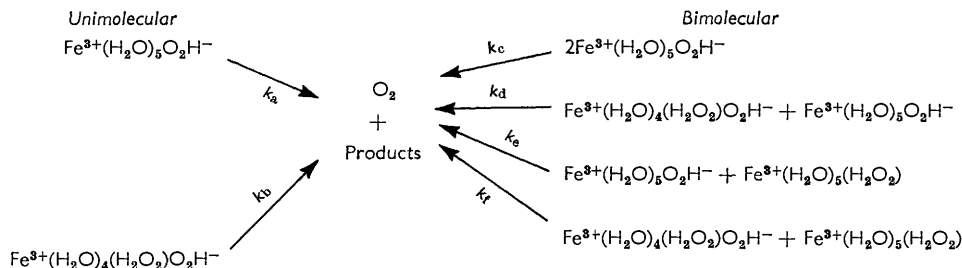
Spectroscopic evidence suggests that the concentration of $Fe^{3+}(H_2O)_4(H_2O_2)_2$ is very small and so its contribution to the decomposition scheme has been omitted. For similar reasons the bimolecular decomposition of $Fe^{3+}(H_2O)_4(H_2O_2)O_2H^-$ has been discounted although its reactions with both the monoperoxy-species have been assumed to make an appreciable contribution.

If these equations represent the decomposition mechanism the rates will depend on the concentrations of the complexes involved and from equation (1) we may say that

$$
-\frac{\mathrm{d}C_{H_2O_2}}{\mathrm{d}t} = \frac{\gamma_a a_{HS}}{\gamma_z \gamma_{H^+}} \left\{ \frac{k_a K_2 K_3 \theta + k_b K_2 K_4 K_5 \theta^2}{(1 + K_2\theta + K_2 K_4 \theta^2)C_{H^+} + \dfrac{\gamma_a a_{HS}}{\gamma_z \gamma_{H^+}}(K_1 + K_2 K_3 \theta + K_2 K_4 K_5 \theta^2)} \right\} C_a
$$

$$
+ \frac{\gamma_a a_{HS}}{\gamma_z \gamma_{H^+}} \left\{ \frac{(k_e K_1^2 K_3^2 \theta^2 + k_f K_2^2 K_4 K_5 \theta^3)C_{H^+} + \dfrac{\gamma_a a_{HS}}{\gamma_z \gamma_{H^+}}(k_c K_2^2 K_3^2 \theta^2 + k_d K_2^2 K_3 K_4 K_5 \theta^3)}{\left[(1 + K_2\theta + K_2 K_4 \theta^2)C_{H^+} + \dfrac{\gamma_a a_{HS}}{\gamma_z \gamma_{H^+}}(K_1 + K_2 K_3 \theta + K_2 K_4 K_5 \theta^2) \right]^2} \right\} C_a^2
$$

$$(12)$$

This equation may be simplified at a number of points:

(1) The term $\gamma_a a_{HS}/\gamma_z \gamma_{H^+}$ has been assumed to be unity.

(2) Spectroscopic evidence has shown that the contribution of the doubly peroxy-substituted species to the ionisation constant is small up to high peroxide concentrations, so that the terms $K_2 K_4 \theta^2$ and $K_2 K_4 K_5 \theta^2$ in the denominators may be neglected without introducing large errors.
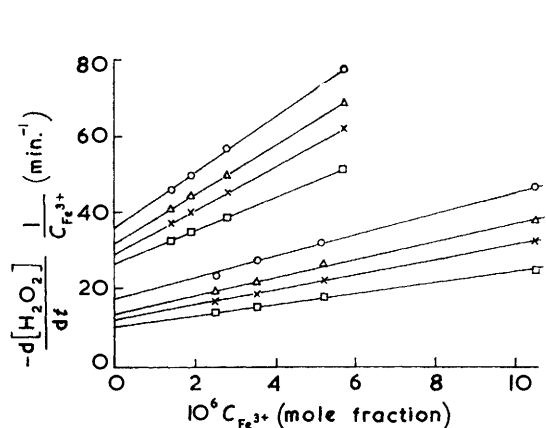
FIG. 5. Plot of $-\dfrac{d[H_2O_2]}{dt} \dfrac{1}{C_{Fe^{3+}}}$ against $C_{Fe^{3+}}$ at $\mu = 0.5$, and $22°$.

$C_{H^+} = \bigcirc, 10^{-2}$M; $\triangle, 1.5 \times 10^{-2}$M; $\times, 2 \times 10^{-2}$M; $\square, 3 \times 10^{-2}$M.

Upper four lines, $\theta = 6.0$.
Lower four lines, $\theta = 0.89$.
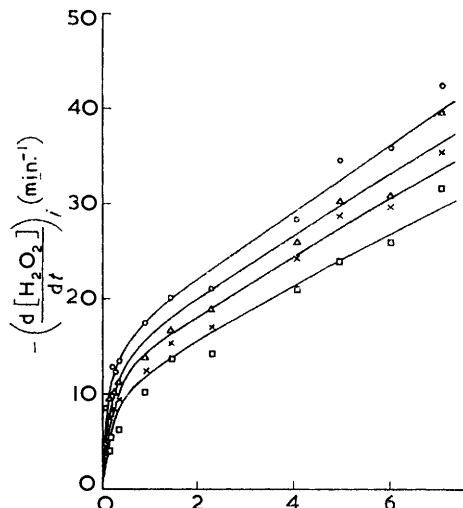
FIG. 6. Plot of $-\left(\dfrac{d[H_2O_2]}{dt}\right)_i$ against θ at $\mu = 0.5$, and $22°$.

Key as Fig. 5. (Curves are calculated values.)
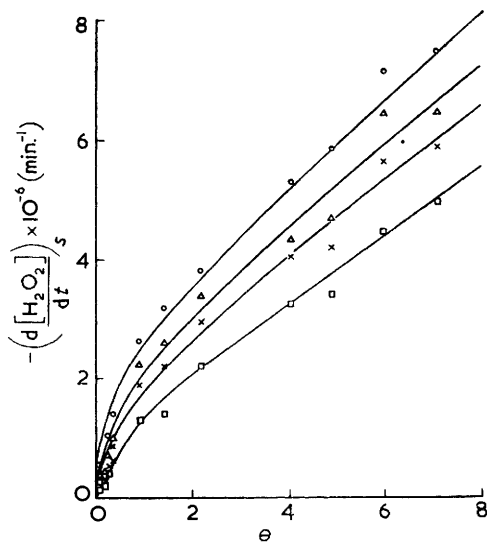
FIG. 7. Plot of $-\left(\dfrac{d[H_2O_2]}{dt}\right)_s$ against θ at $\mu = 0.5$, and $22°$.
Key as Fig. 5.
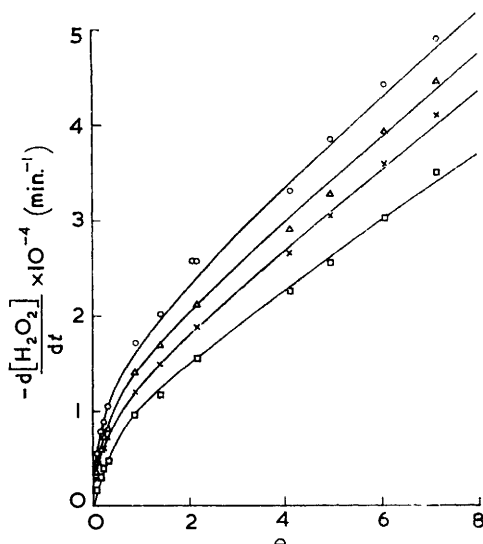
FIG. 8. Plot of $-\dfrac{d[H_2O_2]}{dt}$ against θ at $\mu = 0.5$, and $22°$, with $C_{Fe^{3+}} = 2.62 \times 10^{-4}$M.
Key as Fig. 5.

(3) As K_4 and K_5 could not be determined from the spectroscopic data, they must be included in the appropriate rate constants. Thus $k_b K_4 K_5 = k_B$; $k_f K_4 K_5 = k_F$; and $k_d K_4 K_5 = k_D$.

Under these conditions, equation (12) reduces to

$$-\frac{dC_{H_2O_2}}{dt} = \frac{k_a K_2 K_3 \theta + k_B K_2 \theta^2}{(1 + K_2\theta)C_{H^+} + (K_1 + K_2 K_3\theta)} C_a +$$

$$\frac{(k_e K_2{}^2 K_3 \theta^2 + k_F K_2{}^2\theta^3)C_{H^+} + (k_c K_2{}^2 K_3{}^2\theta^2 + k_D K_2{}^2 K_3\theta^3)}{\{(1 + K_2\theta)C_{H^+} + (K_1 + K_2 K_3\theta)\}^2} C_a{}^2. \quad (13)$$

This equation has been used to interpret the results obtained from the measurements of oxygen evolution.

Results.—Blocks of experiments were performed at constant peroxide concentrations and variable ferric and hydrogen-ion concentrations. Four acid strengths were used throughout the complete range of experiments; they were $C_{H^+} = 1$, $1\cdot5$, 2, and 3×10^{-2}M. Four ferric concentrations were also used at each acidity with $c_a = c_a{}^\circ$, $\frac{1}{2}c_a{}^\circ$, $\frac{1}{3}c_a{}^\circ$, and $\frac{1}{4}c_a{}^\circ$. The absolute value of $c_a{}^\circ$ varied from $2\cdot62$ to $10\cdot67 \times 10^{-4}$M, depending on the peroxide concentration.

If the rate is described by equation (13), then, at constant peroxide and acid concentrations, a plot of $-\frac{1}{c_a} \cdot \frac{dC_{H_2O_2}}{dt}$ against c_a should be linear. The intercept then represents the unimolecular contribution to the rate, and the slope the bimolecular contribution. Such a relationship was found and representative plots are shown on Fig. 5. Figs. 6 and 7 show the change in the unimolecular and the bimolecular components of the rate with θ at the four acid concentrations studied. Fig. 8 shows the change in overall rate at $c_a{}^\circ = 2\cdot67 \times 10^{-4}$M with θ. The similarity of shape of these three curves is striking and will be discussed in the next section.

DISCUSSION

The linearity of the plots displayed in Fig. 5 confirms that the decomposition is mixed uni- and bi-molecular with respect to iron. Measurement of the intercepts of these plots gives the unimolecular contribution which, from equation (13) is equal to

$$-\left(\frac{dC_{H_2O_2}}{dt}\right)_i = \frac{k_a K_2 K_3 \theta + k_B K_2 \theta^2}{(1 + K_2\theta)C_{H^+} + (K_1 + K_2 K_3\theta)}. \quad (14)$$

Thus a graph of $1/\{-(dC_{H_2O_2}/dt)_i\}$ against C_{H^+} at constant θ should be linear, giving an Intercept/Slope $= K_{dec}$, equal to

$$K_{dec} = \frac{K_1 + K_2 K_3 \theta}{1 + K_2\theta}. \quad (15)$$

This equation is identical with that developed in the spectroscopic analysis [equation (9)]. Fig. 9 shows some of the graphs obtained from the four acid concentrations at various peroxide mixtures and Table 4 compares these results with the equivalent from spectroscopic data.

TABLE 4.

Comparison of apparent dissociation constants from spectroscopic and measurements of oxygen evolution.

θ	7·13	6·00	4·90	4·06	2·22	1·39	0·91	0·333	0·233	0·145	0·038
$10^5 K_{sp}$ ...	98, 130	110, 119	108, 138	—	87	77	61, 78	47	30, 35	22	7·5
$10^5 K_{dec}$...	110	140	96	107	78	76	65	35	24	15·7	7·3

Both K_{sp} and K_{dec} exhibit the same trend and the results are generally in reasonable agreement. This agreement justifies the hypothesis that the two species $Fe^{3+}(H_2O)_5 O_2H^-$ and $Fe^{3+}(H_2O)_4(H_2O_2)O_2H^-$ are the sole contributors to the unimolecular decomposition at these peroxide concentrations.

From equation (14) it may be seen that the reciprocal of the intercept in the plot of $1/\{-(dC_{H_2O_2}/dt)_i\}$ against C_{H^+} is given by

$$\frac{1}{i_{dec}} = \frac{k_a K_2 K_3 \theta + k_B K_2 \theta^2}{K_2 K_3 \theta} \text{ (at } \theta \text{ values where } K_2 K_3 \theta \gg K_1).$$

Where there is no contribution from the biperoxy-complex, $1/i_{dec}$ should therefore be independent of θ and only exhibit an increase when this complex begins to become significant in the decomposition. The variation of $1/i_{dec}$ with θ is given in Table 5.

TABLE 5.

Variation of $1/i_{dec}$ with θ.

θ	0·038	0·145	0·233	0·333	0·91	1·39	2·22	4·06	4·9	6·0	7·13
$1/i_{dec}$	21·5	24	32	24	19·5	23·5	25·5	32·6	40·0	37	49

Although the scatter of the results is quite large, a significant increase in the value of $1/i_{dec}$ becomes apparent at $\theta > 2$. This is further confirmation that biperoxy-complexes only appear at high peroxide concentrations. At the lower peroxide range $1/i_{dec} \approx k_a$ and thus, from Table 5, $k_a \approx 22$, expressed in mole fraction units.

The equation for unimolecular decomposition has only two rate constants and various values for these were inserted into the formula to obtain the best fit with the experimental results shown in Fig. 6. Spectroscopic values of K_1, K_2, and K_3 were used for these calculations and the closest agreement was found with values of $k_a = 19·3$ and $k_B = 0·045$. The calculated curves are shown as the solid lines in Fig. 6. It will also be noted that the value of k_a is reasonably close to that obtained by the previous method.

A similar technique was employed to determine the rate constants responsible for the bimolecular reaction. In this case the situation is more complex because four constants seem to be involved and the value obtained should be correspondingly less accurate. Further information may be obtained, however, by extending the acid range studied at a given iron concentration.

At constant peroxide and iron, equation (13) may be expressed as

$$-\frac{dC_{H_2O_2}}{dt} = \frac{A}{BC_{H^+} + C} + \frac{DC_{H^+} + E}{(BC_{H^+} + C)^2},$$

where A, B, C, D, E represent constants.

It may be readily seen that, if $DC = EB$, then the equation reduces to

$$-\frac{dC_{H_2O_2}}{dt} = \frac{A + D/B}{BC_{H^+} + C} \tag{16}$$

and therefore a plot of $1/\{-(dC_{H_2O_2}/dt)\}$ against C_{H^+} should be linear over a wide acid range. We may show further that if $DC < EB$ this plot will result in a curvature away from the C_{H^+} axis, and conversely if $DC > EB$ the curvature will be toward this axis.

Substituting for $D, C, E,$ and B, and if $(k_e K_3 + k_F \theta)(K_1 + K_2 K_3 \theta) < (k_c K_3 + k_D \theta)(K_3 + K_2 K_3 \theta)$, or, from equation (9),

if

$$\frac{k_e K_3 + k_F \theta}{k_c K_3 + k_D \theta} < \frac{K_3}{K_{sp}}, \tag{17}$$

then the plot of $1/\{-(dC_{H_2O_2}/dt)\}$ against C_{H^+} should result in a curvature away from the C_{H^+} axis. The right-hand side of equation (17) is known from the spectroscopic results.

These extended acid runs were performed at $C_a = 2·62 \times 10^{-4}$M over as wide a range as could be conveniently measured. Some of the results obtained are shown in Fig. 10. It was noticed that generally the curvature away from the C_{H^+} axis became more pronounced at the more dilute peroxide range and thus $k_e/k_F < k_c/k_D$. At the higher peroxide concentrations the plots are virtually linear over the experimental acid range, indicating that the sides of equation (17) do not differ greatly.

With these considerations in mind, various values of the four bimolecular reaction constants were inserted into the equation

$$\left(\frac{dC_{H_2O_2}}{dt}\right)_s = \frac{(k_eK_2^2K_3\theta^2 + k_FK_2^2\theta^3)C_{H^+} + (k_cK_2^2K_3\theta^2 + k_DK_2^2K_3\theta^3)}{\{(1 + K_2\theta)C_{H^+} + (K_1 + K_2K_3\theta)\}^2} \tag{18}$$

to obtain the best fit. Closest agreement was obtained with the values, $k_c = 3\cdot3 \times 10^6$, $k_D = 1 \times 10^3$, $k_e = $ zero, $k_F = 1 \times 10^3$, all expressed in mole fraction units.
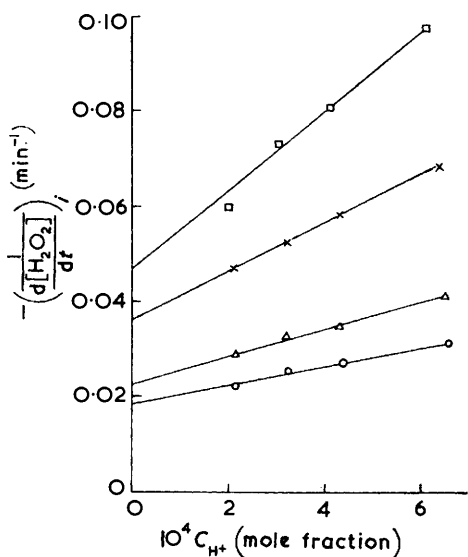
Fig. 9.   Plot of $-\dfrac{1}{\left(\dfrac{d[H_2O_2]}{dt}\right)_i}$ against C_{H^+} at $\mu = 0\cdot5$, and $22°$.

$\theta = \bigcirc, 7\cdot12; \triangle, 4\cdot9; \times, 2\cdot22; \square, 0\cdot91.$
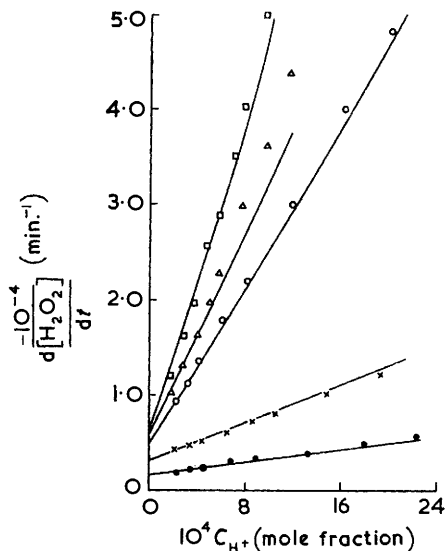
Fig. 10.   Plot of $-\dfrac{1}{\dfrac{d[H_2O_2]}{dt}}$ against C_{H^+} at $\mu = 0\cdot5$, and $22°$, with $C_{Fe^{3+}} = 2\cdot62 \times 10^{-4}$M.

$\theta = \square, 0\cdot145; \triangle, 0\cdot233; \bigcirc, 0\cdot333; \times, 2\cdot22; \bullet, 8\cdot0.$ (Curves are calculated values.)

The plots of the experimental bimolecular rates against θ at various acidities are shown in Fig. 7, where the solid lines are the calculated curves obtained with these values. Fig. 8 shows the overall rate versus θ at $c_a = 2\cdot6 \times 10^{-4}$M at these same acidities, and again the solid lines are curves calculated from equation (13) by using the rate constants evaluated. The agreements are seen to be reasonably good, in view of the wide range of peroxide concentrations studied. This agreement also holds over the extended acid ranges, as demonstrated by the solid lines in Fig. 10. Table 6 lists the constants determined in these series of experiments.

TABLE 6.

Equilibrium constants and rate constants (mole fraction units; at $\mu = 0\cdot5$, and $22°$).

K_1	$2\cdot8 \times 10^{-5}$	k_a	$19\cdot3$	k_D	$1\cdot0 \times 10^3$
K_2	$1\cdot8$	k_B	$4\cdot5 \times 10^{-3}$	k_e	Zero
K_3	$1\cdot1 \times 10^{-3}$	k_C	$3\cdot3 \times 10^6$	k_F	$1\cdot0 \times 10^3$

Conclusions.—Both the spectroscopic and oxygen evolution results confirm the presence of $Fe^{3+}(H_2O)_5O_2H^-$ and $Fe^{3+}(H_2O)_4(H_2O_2)O_2H^-$ in solutions of ferric ions in water–hydrogen peroxide mixtures. These species have been shown to be the sole contributors to the unimolecular decomposition of hydrogen peroxide.

It will be seen both from the experimental curves and from equation (13) that the fractional contribution of the bimolecular component of the reaction to the overall decomposition rate decreases with decreasing peroxide concentration, and so its contribution at very dilute peroxide may be regarded as being very small. This is in agreement with a number of authors who have worked in this region [1] and have found the kinetics to be expressed by the relationship

$$ - \frac{dC_{H_2O_2}}{dt} = \frac{k_0 C_{H_2O_2} C_a}{C_{H^+} + K_1}; $$

at very dilute peroxide, equation (13) reduces to

$$ - \frac{dC_{H_2O_2}}{dt} = \frac{k_a K_2 K_3 C_{H_2O_2} C_a}{C_{H^+} + K_1}, $$

in complete agreement with this formula.

Probably one of the more significant observations to arise from this work is that, in order to explain the results consistently, one has to assume the term $\gamma_a a_{HS}/\gamma_z \gamma_{H^+}$ to be equal to unity. Now the quotient a_{HS}/γ_{H^+} is a measure of the change in basicity of the solvent with composition and is independent of the nature of the solute. Wynne-Jones and his co-workers have shown by glass-electrode [17] and by indicator measurements [18] that the basicities of mixtures of water and hydrogen peroxide decrease by several powers of ten as the solvent composition changes from water to very concentrated peroxide.

Therefore in order to maintain the constancy of the expression $\frac{\gamma_a a_{HS}}{\gamma_z \gamma_{H^+}}$, $\frac{\gamma_a}{\gamma_z}$ must increase proportionately. Similar assumptions have to be made in the analysis of the decomposition kinetics of hydrogen peroxide catalysed by chromium and molybdenum.[14]

Work on the basicities of these solvent mixtures is continuing.

MINISTRY OF AVIATION, EXPLOSIVES RESEARCH & DEVELOPMENT ESTABLISHMENT,
WALTHAM ABBEY, ESSEX.

[17] Mitchell and Wynne-Jones, *Trans. Faraday Soc.*, 1955, **51**, 1690.
[18] Beck and Wynne-Jones, *J. Chim. phys.*, 1952, **49**, C, 97.